

Electronic Supporting Information

Lequan Liu,^{abc} Peng Li,^d Tao Wang,^c Huilin Hu,^{ab} Haiying Jiang,^c Huimin Liu,^c Jinhua Ye^{abcd}

^a TU-NIMS Joint Research Center and Tianjin Key Laboratory of Composite and Functional Materials, School of Material Science and Engineering, Tianjin University, 92 Weijin Road, Tianjin (P.R. China);

^b Collaborative Innovation Center of Chemical Science and Engineering (Tianjin), Tianjin 300072, People's Republic of China;

^c International Center for Materials Nanoarchitectonics (WPI-MANA), National Institute for Materials Science, (NIMS) 1-1 Namiki, Tsukuba, Ibaraki 305-0044 (Japan);

E-mail: jinhua.ye@nims.go.jp

^d Environmental Remediation Materials Unit, National Institute for Materials Science (NIMS) 1-1 Namiki, Tsukuba, Ibaraki 305-0044 (Japan);

Material Preparation

SrTiO₃ nanoparticles were prepared with a modified Polymerized Complex (PC) method which has been described in our previous work. Briefly, strontium and titanium precursors were dissolved in 2-methoxyethanol respectively, and then were mixed together. Polymerization was carried out after introducing of citric acid and ethylene glycol. Organic frames were totally removed by calcinations at 500 °C. Au/SrTiO₃ photocatalysts was prepared with deposition-precipitation method by using urea (CO(NH₂)₂) as the precipitating base. After being washed with high pure water and dried at 60 °C overnight, the powder either calcined at 650 °C for 2h to get Au/SrTiO₃, or homogeneous mixed ST01 with mole ratio of 1:2 (SrTiO₃:TiO₂) by using an agate mortar and then calcined at 650 °C for 2h to form Au/SrTiO₃/TiO₂ composite photocatalyst. For comparison, Au/TiO₂ and Au/TiO₂/SrTiO₃ (SrTiO₃:TiO₂:2:1) were prepared with similar procedure by using the same TiO₂ and SrTiO₃ semiconductors.

Sample Characterization

High-resolution transmission electron microscopy (TEM) characterization was performed with a JEOL 2100F operated at 200 kV. Powder X-ray diffraction (XRD) patterns of the products were recorded on an X'Pert PRO diffractometer with Cu-K α radiation. The Brunauer-Emmett-Teller (BET) surface areas were measured via nitrogen physisorption (Gemini-2360; Micromeritics Corp., U.S.A.). UV-vis diffusion

reflectance absorption spectra were recorded with a Shimadzu UV-2600, where an integrating sphere was used in diffusion reflectance absorption analysis. X-Ray Photoelectron Spectroscopy (XPS) experiments were performed in a Theta probe (Thermo Fisher) using monochromated Al K α X-rays. Raman spectra were obtained on NRS-1000 Laser Raman Spectrophotometer (Jasco Inc., Japan) with a laser source at 532 nm. Steady state and dynamic PL of samples were measured using an excitation wavelength of 335 nm and a 330nm diode laser, respectively, on a Fluorolog-3 spectrofluorometer (Horiba Jobin Yvon). The experiments were carried out under ambient conditions. Actual Au loadings were obtained by inductively coupled plasma optical emission spectrometry (ICP-OES, SPS3520UV-DD, SII nano technology Inc., Japan). Theoretical and actual Au loading amounts of Au/SrTiO₃ prepared with deposition-precipitation (DP) method are 1.5% and 1.1% respectively, while the corresponding values of Au/SrTiO₃/TiO₂ are 0.59% and 0.58% respectively. For Au/TiO₂ (DP method), theoretical and actual Au loading amounts are 1.5% and 1.2% respectively, while the corresponding values of Au/TiO₂/SrTiO₃ are 0.56% and 0.55% respectively.

Electrochemical impedance spectroscopy (EIS) measurements were carried in a quartzose beaker and an electrochemical station (ALS/CH model 650A) at frequencies between 100 kHz and 0.1 Hz. The amplitude of the sinusoidal potential signal was 5 mV. A coated ITO is as the working electrode, a platinum foil as the counter electrode, and saturated calomel electrode (SCE) electrode as the reference electrode in 0.5 M Na₂SO₄ aqueous solution. For working electrodes, 5 mg of photocatalyst and 50 μ L of Nafion solution (5 wt%) were dispersed in 1 mL of ethanol to form a homogeneous turbid liquid and then 100 μ L of turbid liquid was deposited on ITO conductive glass with an area of 1 cm². A 300 W Xenon arc lamp with a L-42 glass filter was used as the light source.

Activity Evaluation

For iso-propanol (IPA) photocatalytic degradation, typically, certain amount of Au/SrTiO₃, Au/TiO₂, Au/SrTiO₃/TiO₂, Au/TiO₂/SrTiO₃ catalysts (corresponding to 3.9 μ mol Au) were spread uniformly in a quartz-made vessel with an irradiation area of 9.0 cm². The CO₂-containing natural air sealed in the vessel was replaced by \sim 1 atm of artificial pure air (O₂/N₂=1/9). Then, a certain amount of gaseous IPA was injected into the vessel. Prior to light irradiation, the vessel was kept in dark for 2 h until an adsorption-desorption equilibrium was finally established. The visible-light (420 nm < λ < 910 nm) was obtained by using combination of Y44+R900 filters and a water filter. The products were analyzed with a gas chromatograph system (GC-2014, Shimadzu, Japan) with a flame ionization detector (FID).

Photocatalytic O₂ evolution was carried out with photocatalyst suspended in 270 ml water in the presence of 5 mmol AgNO₃ as sacrificial reagent. A 300W Xe arc lamp was employed as the light source. For visible-light ($\lambda > 400$ nm) reaction, a L42 cutoff filter was used to remove UV light. The concentrations of O₂ were detected by the gas chromatograph (GC-8A with TCD, Shimadzu).

Recyclability studies of IPA degradation was carried out by purging the reactant as well as products by artificial pure air, and then IPA was injected into the system for second evaluation. Recyclability studies of O₂ evolution was carried out by evacuate the produced O₂ and evaluated for the second time without adding any reactant.

Detection of reactive oxygen species

•O₂⁻ radical was studied with Electron spin resonance (ESR) carried out with JEOL JES-FA-200 at 4.2 K achieved with liquid helium. The samples after treated with air at room temperature in the dark or visible light irradiation ($\lambda > 420$ nm) was subjected to evaluation.

The concentration of H₂O₂ formed during the photocatalytic process was determined by the DPD method. DPD solution: 0.1g N, N-Diethyl-1,4-phenylenediammonium sulfate (DPD) was dissolved in 10 ml 0.05 M H₂SO₄; POD solution: 10 mg Peroxidase (POD) Horseradish was dissolved in 10 ml ultrapure water (Direct-Q3 UV); Buffer: 0.1 M Na₂HPO₄ and NaH₂PO₄ solution with the target pH value of 6.0. Photocatalyst was dispersed in an aqueous solution composing of 27 ml deionized water, 3 ml phosphate buffer, 50 μ L of POD and 50 μ L of DPD solutions, and 12 μ L methanol. The suspension was irradiated with visible-light ($\lambda > 420$ nm) after being stirred for 10 mins in dark. The absorbance of the solution at 551 nm was recorded using a spectrophotometer (Shimadzu UV-2500).

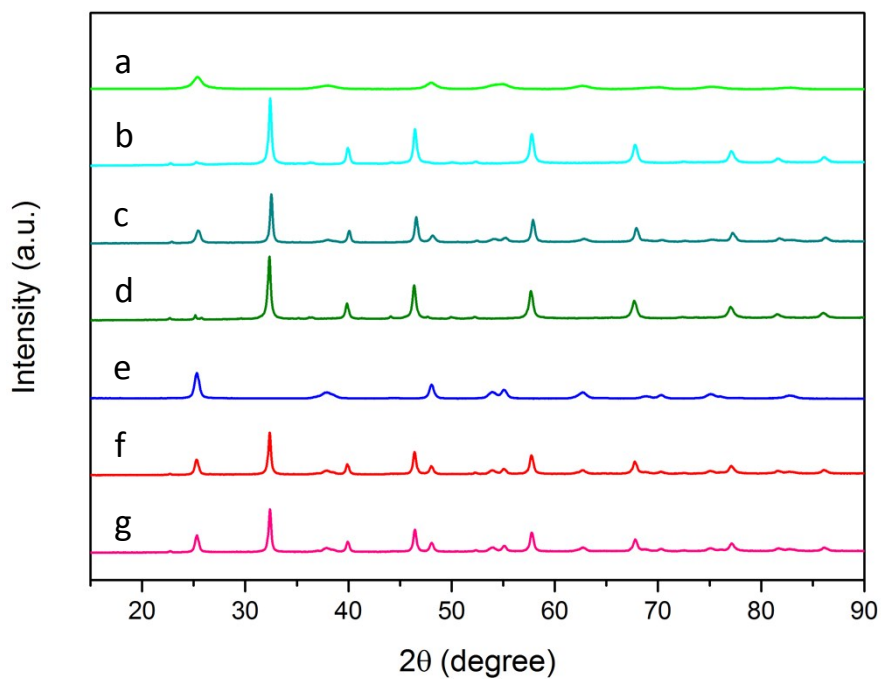


Fig. S1. XRD patterns of TiO_2 (a), SrTiO_3 (b), $\text{SrTiO}_3/\text{TiO}_2$ (c), Au/SrTiO_3 (d), Au/TiO_2 (e), $\text{Au}/\text{SrTiO}_3/\text{TiO}_2$ (f) and $\text{Au}/\text{TiO}_2/\text{SrTiO}_3$ (g).

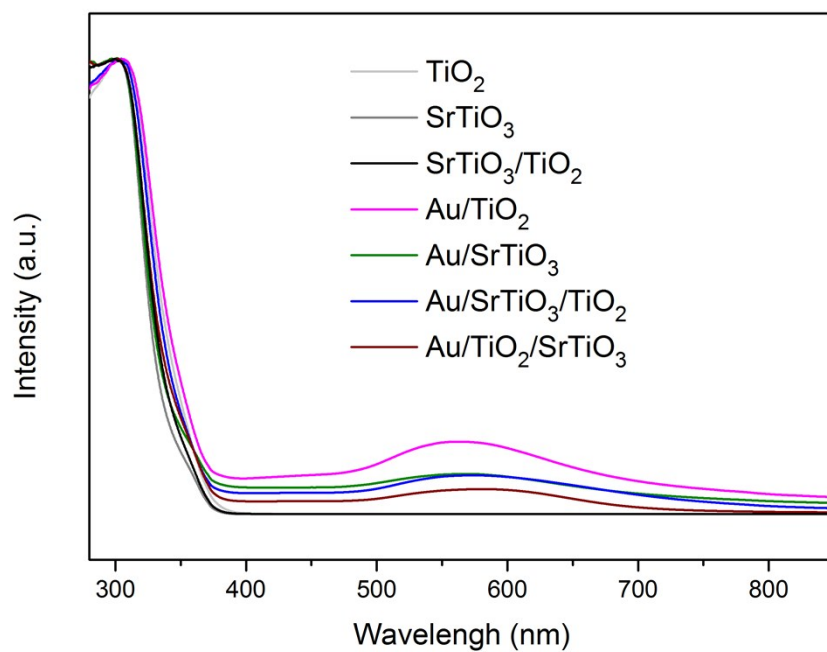


Fig. S2. Normalized UV-vis diffusion reflectance absorption spectra of composite materials

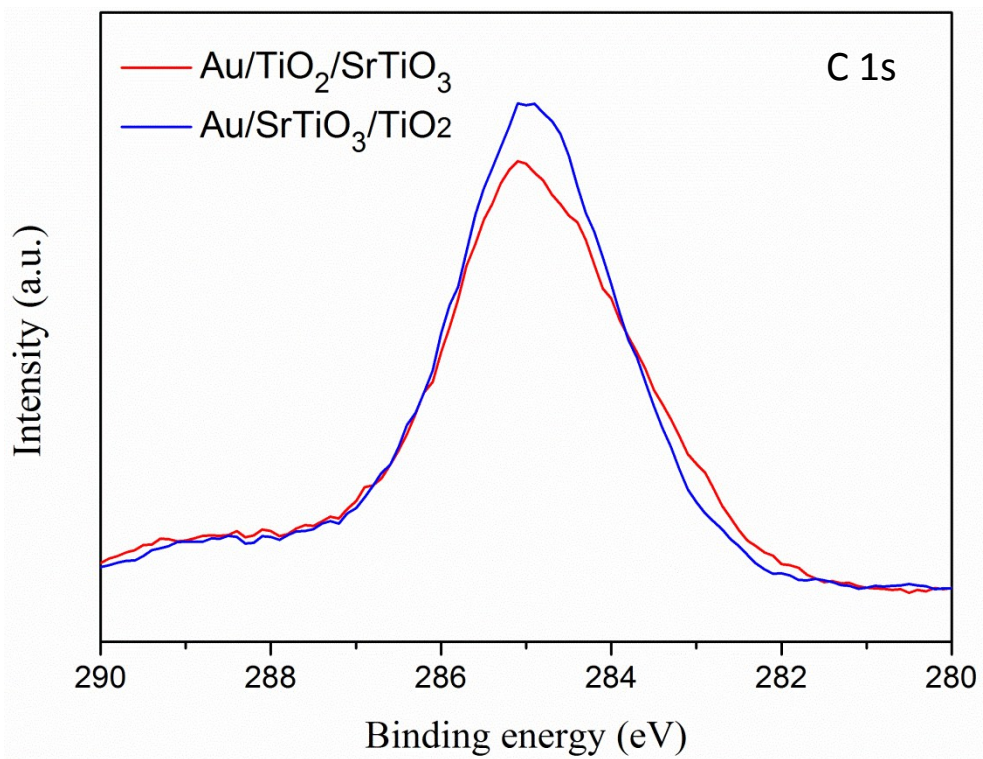
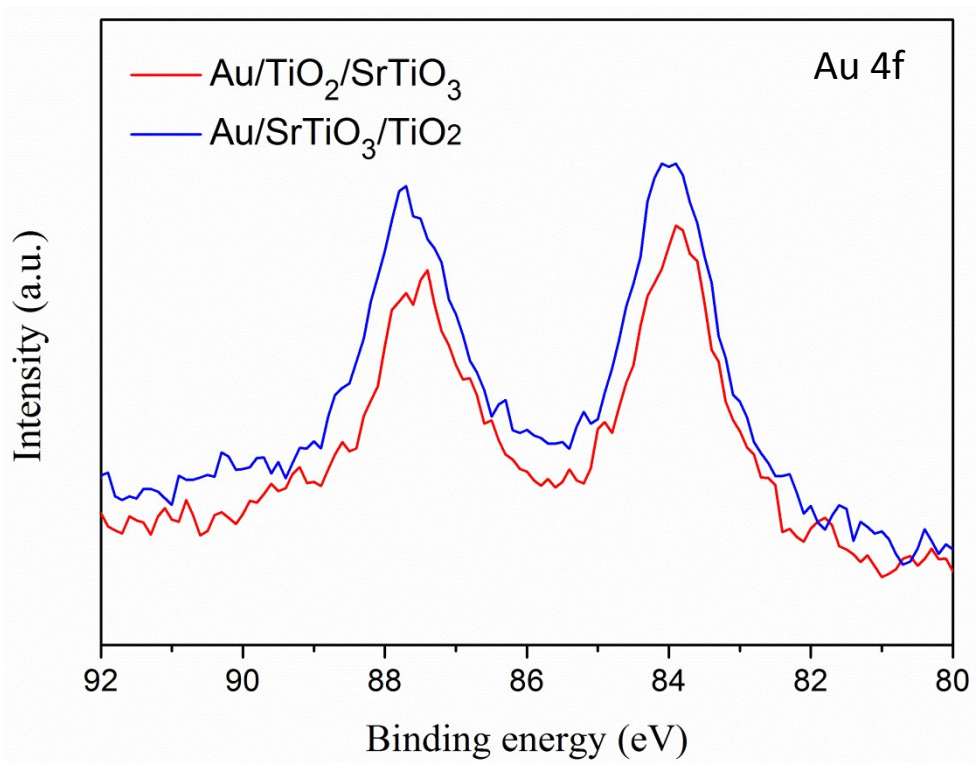


Fig. S3. XPS binding energy of Au 4f and C 1s in Au/SrTiO₃/TiO₂ and Au/TiO₂/SrTiO₃

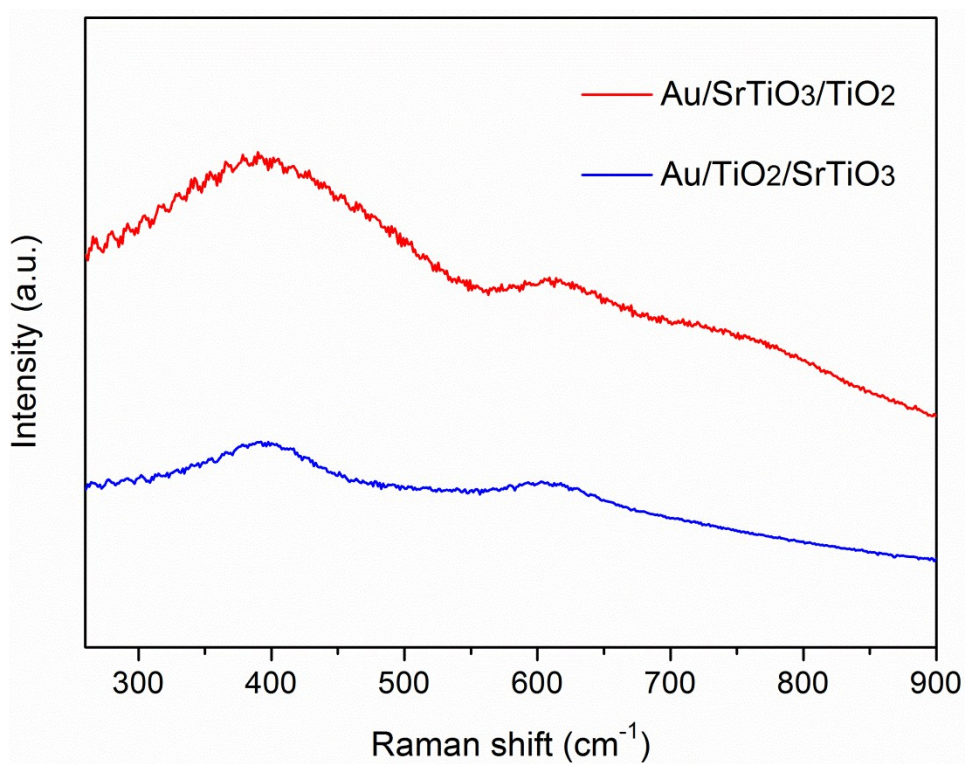


Fig. S4. Raman scattering spectra of Au/SrTiO₃/TiO₂ and Au/TiO₂/SrTiO₃.

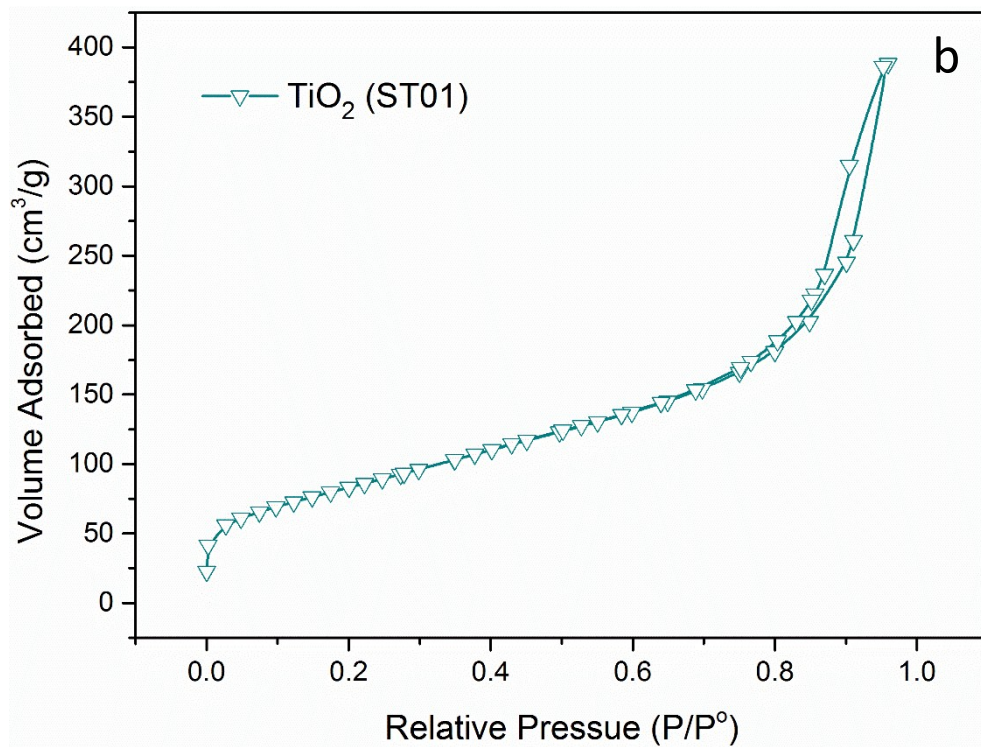
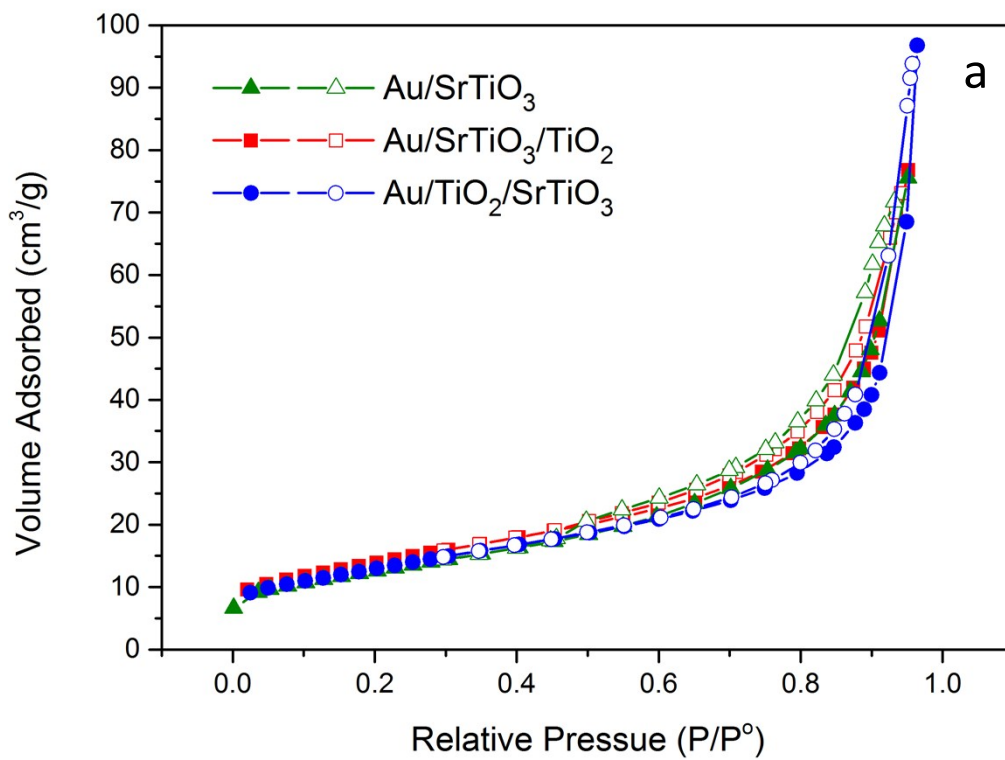


Fig. S5. Nitrogen physisorption isotherms of Au/SrTiO₃, Au/SrTiO₃/TiO₂ and Au/TiO₂/SrTiO₃ a) and TiO₂ (ST01), b).

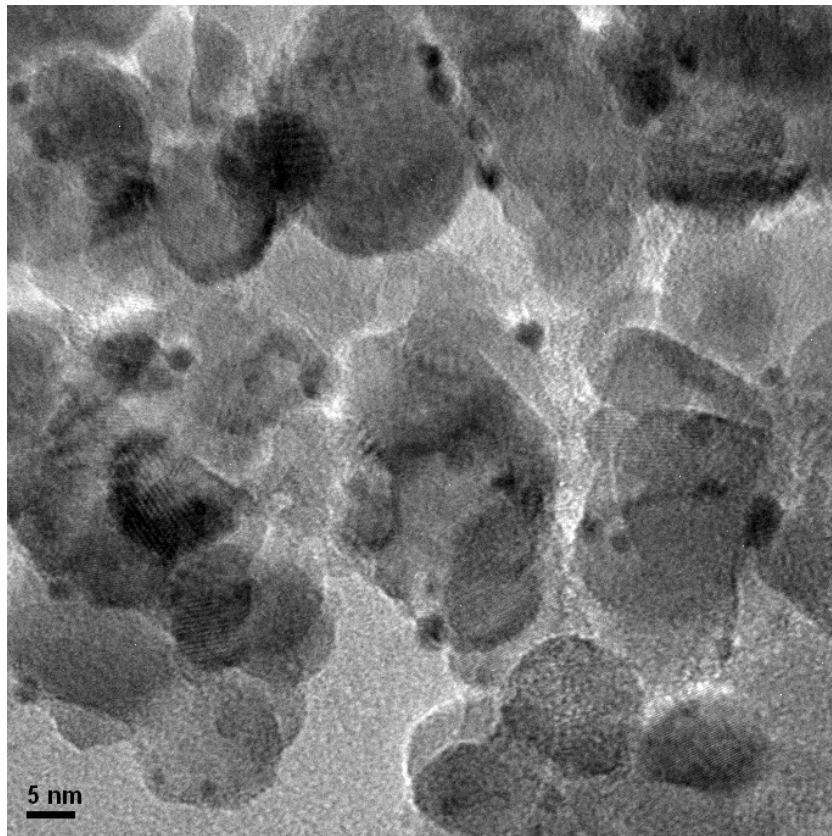


Fig. S6. Representative TEM image of Au/SrTiO₃.

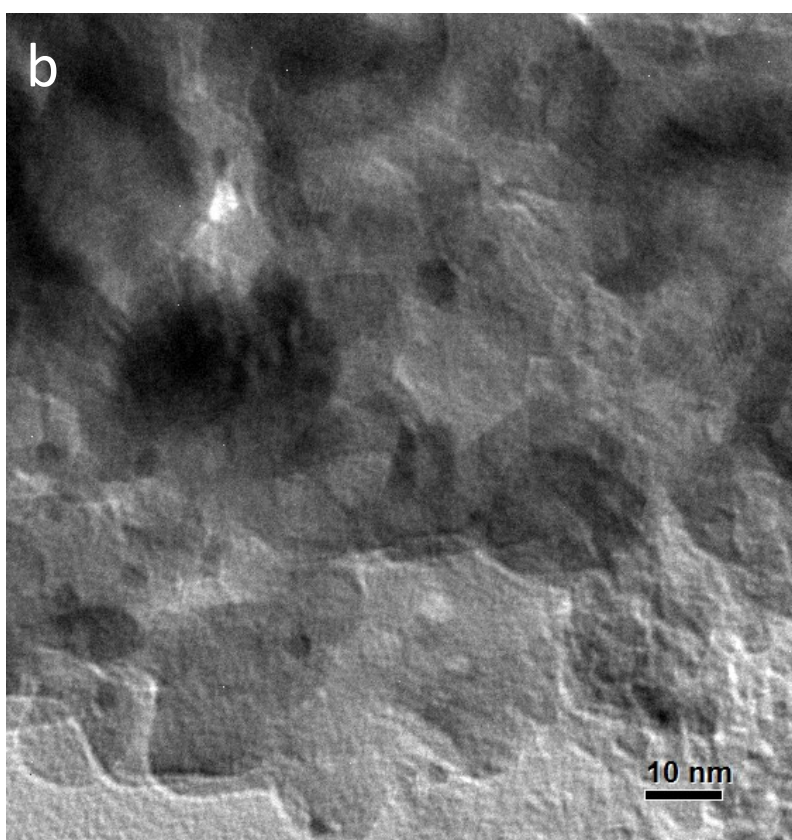
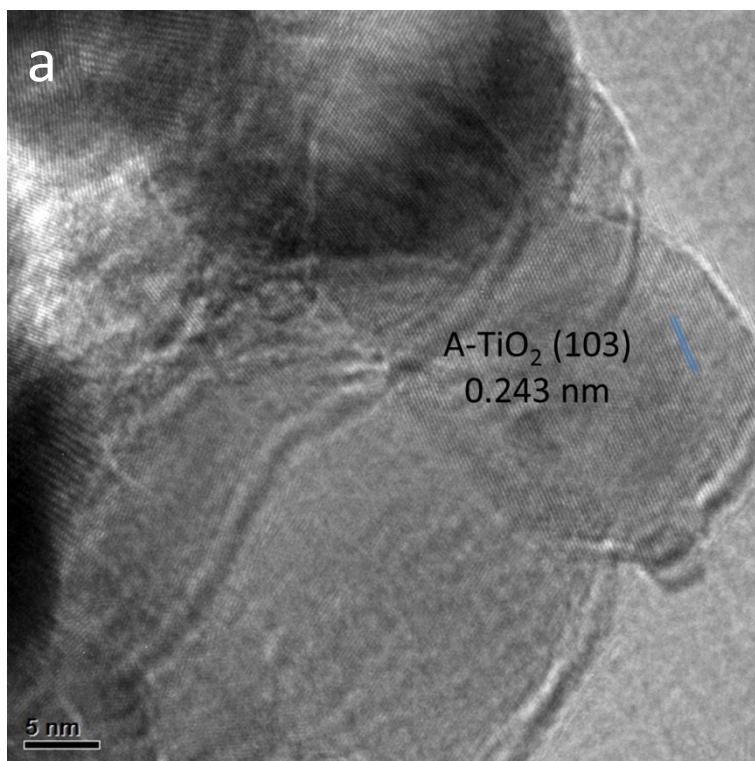


Fig. S7. Representative TEM images of Au/TiO₂/SrTiO₃.

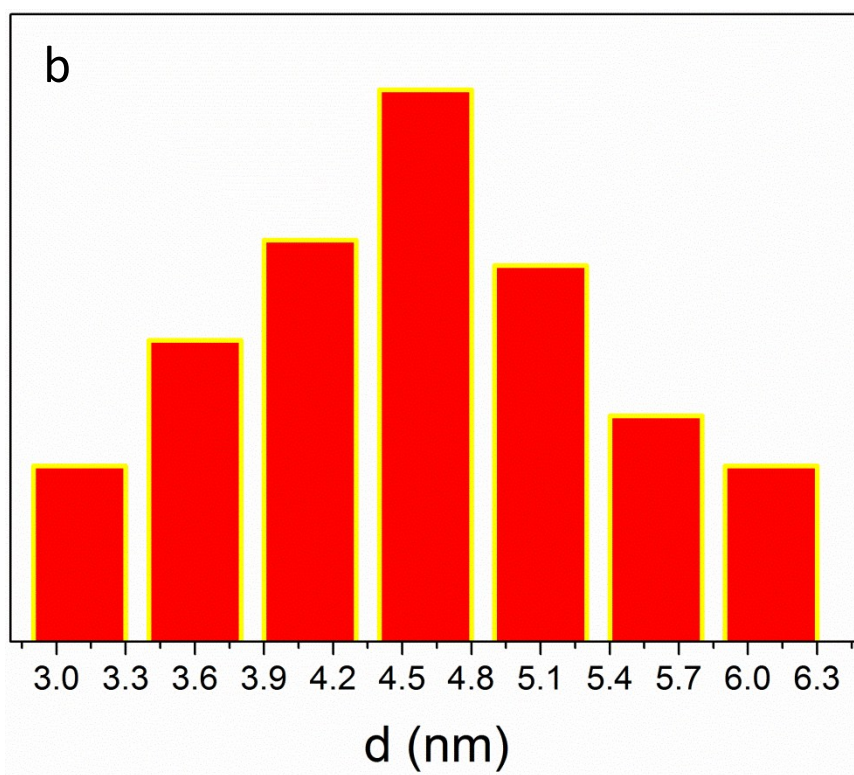
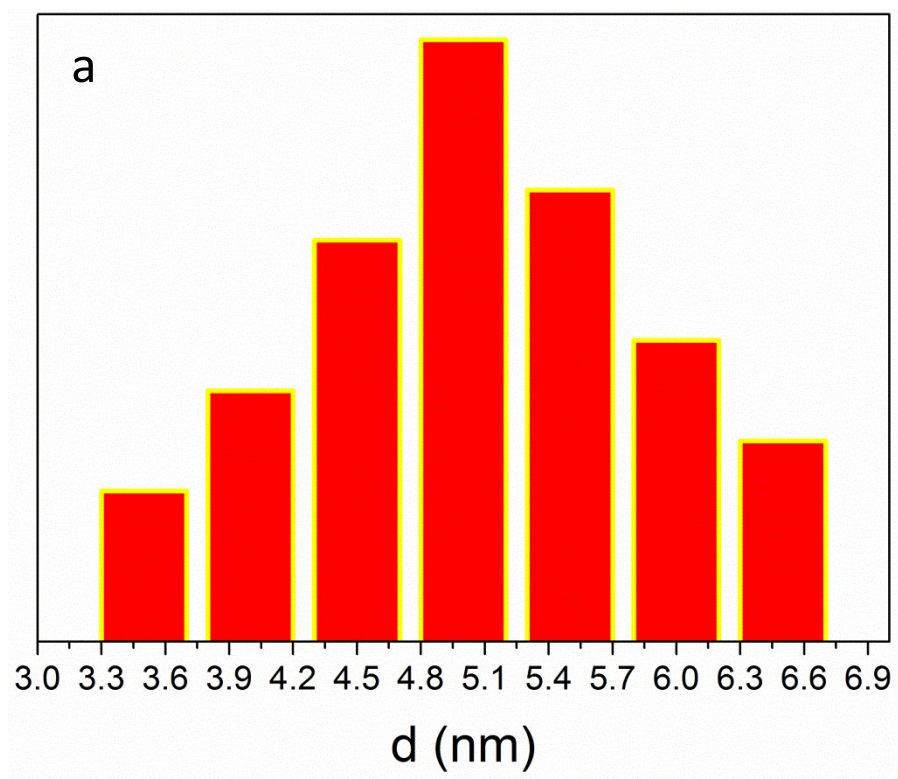


Fig. S8. Au size distribution histograms of Au/SrTiO₃/TiO₂ (a) and Au/TiO₂/SrTiO₃ (b) obtained by counting about 50 particles.

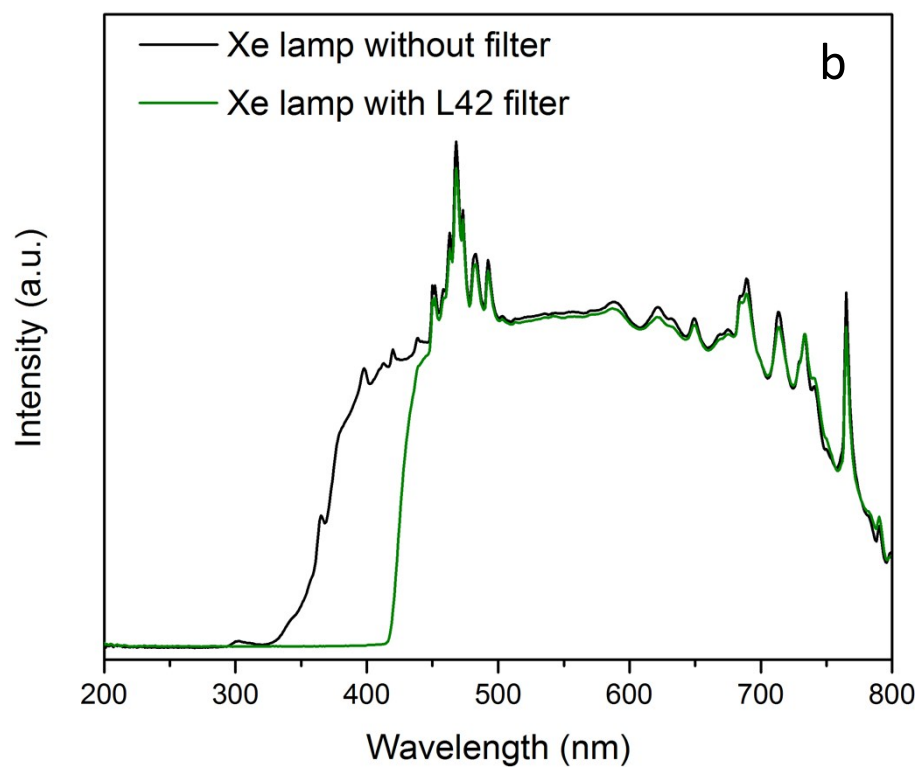
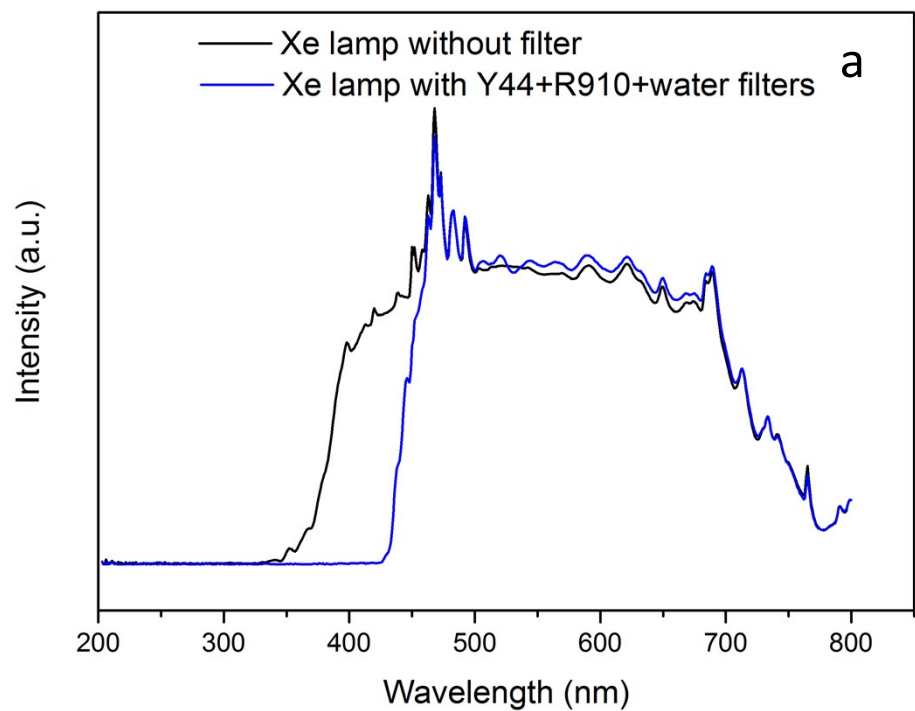


Fig. S9 Light spectra of Xe lamp with and Y44+R910+water filters (a) and L42 filter (b).

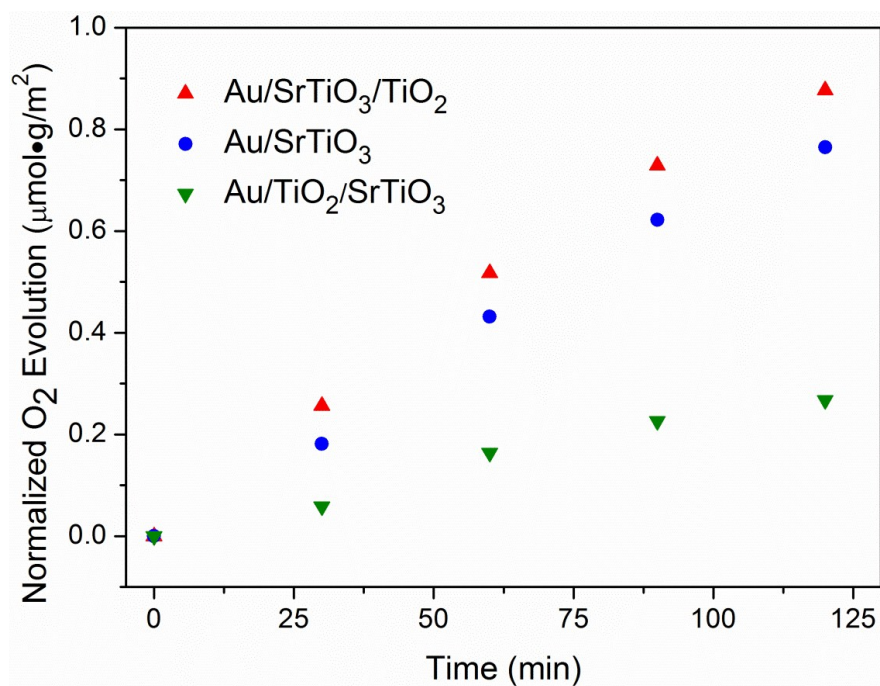


Fig. S10 Visible-light O₂ evolution rates normalized with corresponding surface area over Au/SrTiO₃/TiO₂, Au/SrTiO₃ and Au/TiO₂/SrTiO₃.

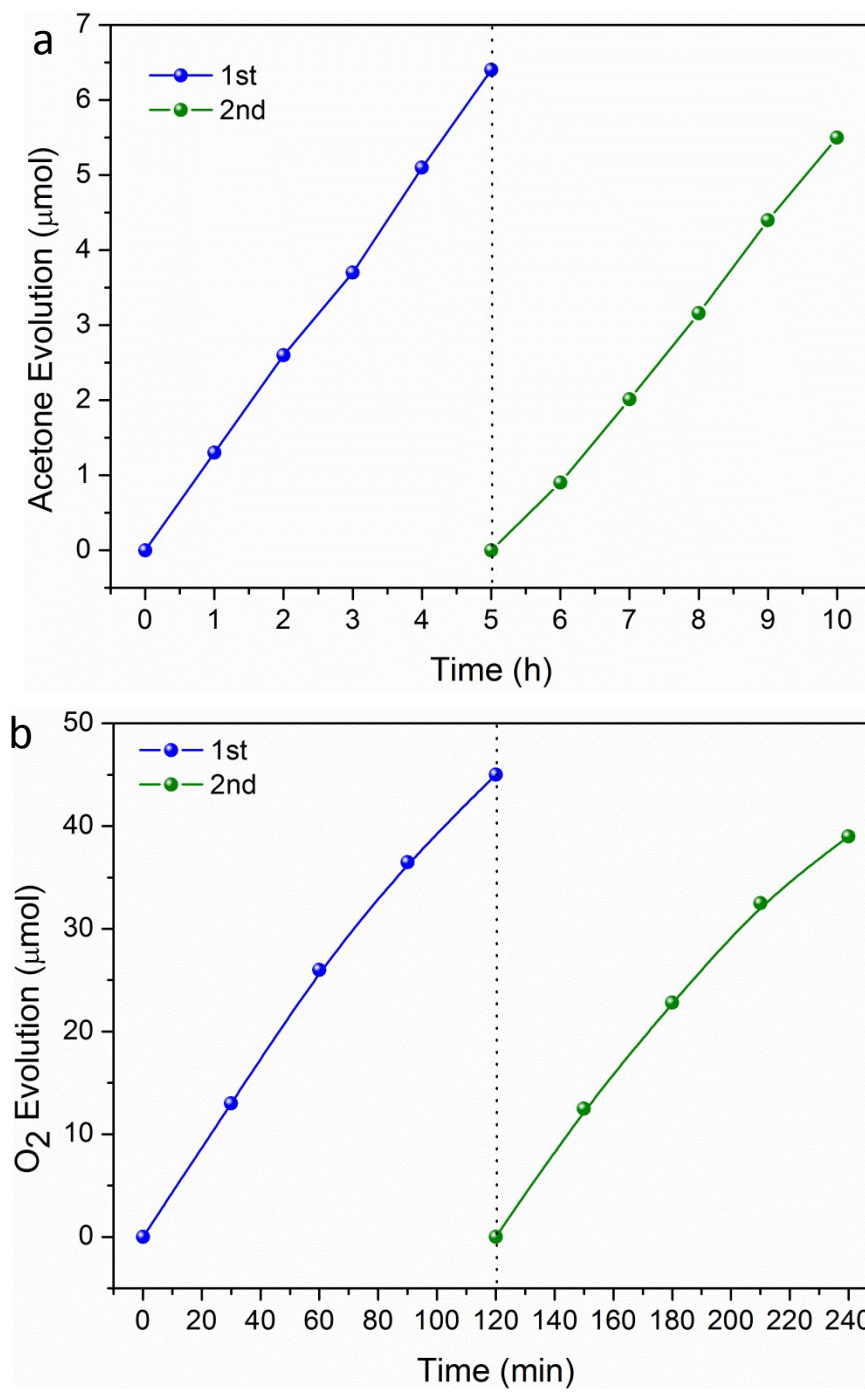


Fig. S11 Recyclability studies over Au/SrTiO₃/TiO₂ in degradation of IPA (a) and O₂ evolution (b).

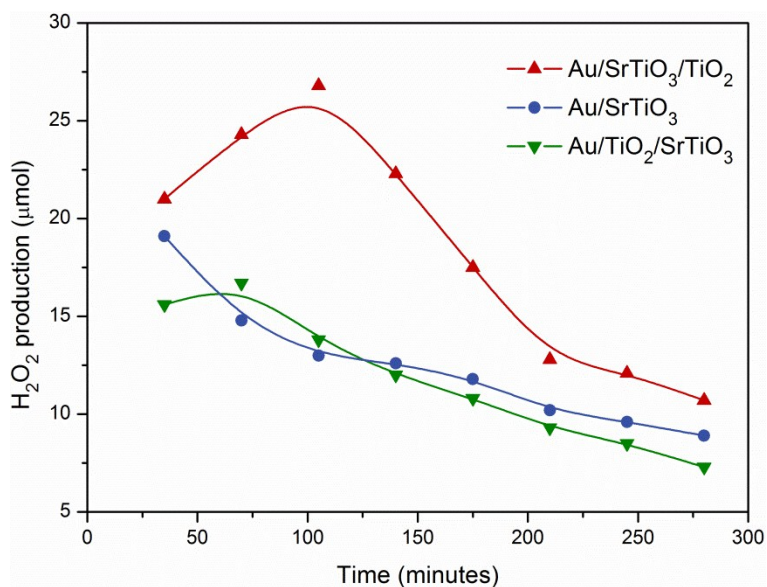


Fig. S12 Generation of H₂O₂ during irradiation of Au/SrTiO₃ and Au/SrTiO₃/TiO₂ under visible light ($\lambda > 420$ nm). The concentration of H₂O₂ formed during the photocatalytic process was determined by the DPD method.

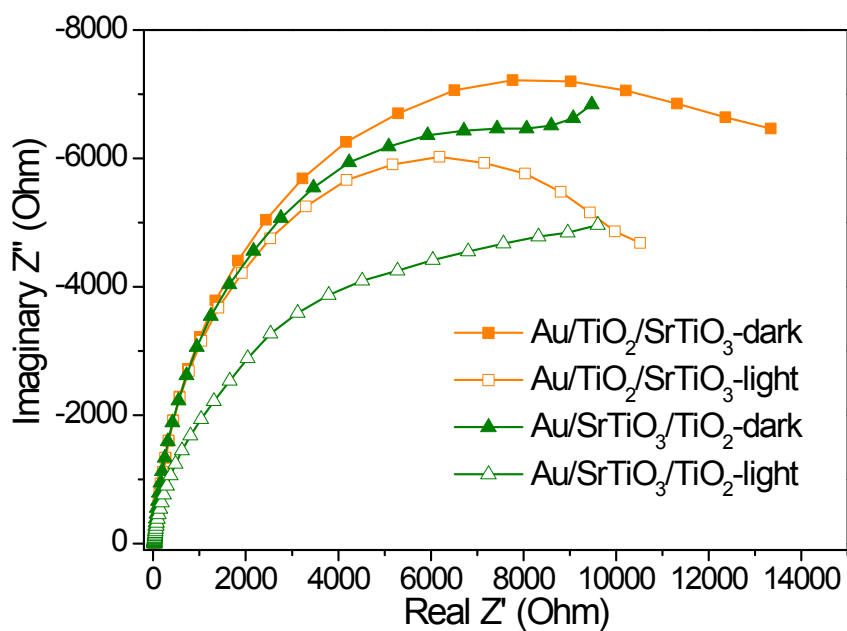


Fig.S13 Electrochemical impedance spectroscopy (EIS) Nyquist plots of Au/SrTiO₃/TiO₂ and Au/TiO₂/SrTiO₃ composites.